Bottom-Up Approach to Innovative Memory Devices: II. Molecular Adsorption on Electrodes and the Asymmetric Response

Ilaria Pino,*,†,¶ Mauro Causà,† and Vincenzo Barone‡,¶,||

Dipartimento di Chimica, Università di Napoli."Federico II", Complesso di Monte S. Angelo, Via Cintia, I-80126 Napoli, Italy, and Scuola Normale Superiore, Piazza dei Cavalieri 7, 56126, Pisa, Italy

Received: July 8, 2010; Revised Manuscript Received: October 12, 2010

The 50 nm-thick polystyrene (PS) film, involved in some innovative memory devices, is sandwiched between two Al electrodes and contains 8-hydroxyquinoline (8HQ) molecules and gold nanoparticles. A periodic DFT study of the molecular adsorption of two different tautomers of the 8HQ on an Al (111) surface has been performed. The changes of the metal work function under molecular adsorption have been calculated to determine the possible effect at the interface on the electron and hole injection barriers. The strong adsorption of the 8HQ(II) tautomer makes the work function change up to 1.2 eV with respect to the bare Al (111) surface. Hence, the stabilization of the 8HQ(II) at the interface could play a key role in the switching mechanism of the device.

Introduction

Bistable organic electronic devices are very promising for applications in several fields of current technological interest, such as nonvolatile computer memories.[1−5] Yang and co-workers describe an organic memory device, constituted by a sandwich structure, namely a solid polystyrene (PS) solution containing dodecanethiol-capped gold nanoparticles (AuNP) and 8-hydroxyquinoline (8HQ) molecules, between aluminum electrodes.[6] The most interesting characteristics of this class of devices is the amazing simplicity of their structure, and thus the economic advantage in their production with respect to conventional semiconductor-based memory devices that comprise many layers of different materials. It is also important to take into account the environmental advantages of organic electronic components in terms of their lower energy content and of the less hazardous chemicals involved in their preparation.

The first characteristic of the Yang's device, the so-called bistability, which allows the apparatus to be used as a memory device, and to classify it under the FET (field-effect-transistor) family, is the ability to switch from a low-conductivity state to a high-conductivity one by the application of low bias at the aluminum electrodes. The second feature is a large hysteresis width in the current−voltage plot, which implies a sharp-cut electric current difference between the two conductivity regimes when a specific voltage is applied. This characteristic permits to obtain a good accuracy and reliability on reading the Boolean information about the conductivity state. In this way, it is possible to exploit the device as a write/read/erase memory, as long as three specific voltages can be chosen in order to write (switch on), read, and erase (switch off) the information (current flow). The third requirement is the qualitative and quantitative stability of the device properties under thousands of switching iterations (write/read/erase cycles). Indeed, under the application of at least 2.8 V for less than 25 ns, the current intensity flowing through the memory device increases from 10^{-11} to 10^{-6} A, whereas at positive voltages lower than 2.8 V the device remains in its conductivity regime, either high or low.[6] The application of an inverse bias of at least −1.8 V is required to make it switch back to its high-resistance regime.

A deeper understanding of the key physical/chemical factors tuning the behavior of organic electronic devices is a mandatory prerequisite for optimizing the structure and the composition of the materials, for approaching the performances, the stability, and the reliability of the corresponding semiconductor devices, or even for new components.[7] The present study represents the second step[8] of a project aimed at understanding the various aspects of the Yang's device, using the tools of computational chemistry. Our first aim is to describe the low-conductivity regime of the device, throwing light on the thermodynamics to be obeyed for electronic switching to the high-conductivity state. The first requirement for the electric current to flow through the device is electron or hole injection from metal electrodes to the polymeric film.[9−12] It has been assessed from experimental evidence that the mean conductive molecular component is represented by the 8HQ molecules, which determine the voltage thresholds at the aluminum interfaces,[4,6] whereas the hysteresis width and the $I-V$ asymmetric behavior are caused by the presence of AuNPs and are sensitive to their concentration and size. In other recent experimental works,[13,14] a direct proportionality between the switching voltages, the conductivity, and the concentrations of gold nanoparticles and 8HQ molecules in a polystyrene matrix have been measured. At concentrations lower than a certain percolation threshold, the current is due to electrons passing from the metal electrodes through the insulating composite. Near and above the percolation threshold, and for the application of a critical voltage, charge transport is likely to take place between 8HQ molecules.

In the first part of this study,[8] the calculations of the structural and electronic properties of the PS−8HQ mixture uncovered the role that PS-solvation plays in lowering both the hole and the electron injection barriers, determining the voltage to be applied for the conductivity switching. The latter aim was achieved by calculating the electron affinities (EA) and ioniza-

* To whom correspondence should be addressed. E-mail: i.pino@chem.leidenuniv.nl.
† Università di Napoli.
‡ Scuola Normale Superiore.
¶ Leiden Institute of Chemistry, Leiden University, Einsteinweg 55, 2333CC Leiden, The Netherlands.
|| INFN - Sezione di Perugia, via A. Pascoli, 06123 Perugia, Italy.

10.1021/jp1063287
Published on Web 11/10/2010

tion potentials (IP) of the 8HQ molecules in this specific environment and by considering the experimental value of the aluminum work function. However, we neglected possible aluminum surface alterations, due to molecular periodic adsorption which often modifies considerably the metal work function, depending on the nature of the ad-molecules and on the coverage degree of the surface.[15−17] In this work, we present a quantum mechanical (QM) study of the adsorption of 8HQ in its two tautomeric forms on the Al (111) surface, and we show how the relative work function modifications provide information about the conduction mechanism. In particular, we address the following questions: (i) Can 8HQ molecules adsorb on the Al (111) surface? (ii) Does the Al electrode work function change under 8HQ adsorption?

The present work is organized as follows: The second section provides a brief account of the computational methods and theoretical models. In the third section we discuss the issue of the injection mechanisms and the variables involved. In the fourth section, the main computational results for 8HQ adsorption on the Al (111) surface are analyzed, and in the fifth section, conclusions are presented.

Computational Methods

Periodic DFT calculations were performed on slabs (2-D periodicity) with the CRYSTAL06 program.[18,19] The infinite series of Coulombic integrals was approximated with Ewald techniques,[20] whereas the infinite exchange series, representing an essentially short-range interaction, was truncated to ensure convergence for energy and related observables.[21] The solution of the effective one-electron Schrödinger equation was performed in reciprocal space sampling k points on a regular mesh.[22] The symmetry was fully implemented in direct space, to minimize the number of molecular integrals that needed to be computed and stored, and in reciprocal space, to perform a block diagonalization.[23] Energy derivatives with respect to the position of the atoms in the unit cell were implemented,[24−26] thus making it possible to optimize the equilibrium geometry within a given crystal symmetry by an effective quasi-Newton technique.

Surfaces and adsorption were studied by means of 2-D periodic supercells. The substrate was represented by a slab of atomic layers. The use of only 2-D translational symmetry allows one to study surfaces with models that have an infinite vacuum above them; this avoids the complicated problem of defining the potential at infinity. The use of dummy layers above the surface allowed an improvement on work functions.

The hybrid gradient-corrected B3LYP[27] density functional was used at the all-electron level using an optimized 88-31G* basis set for the Al atoms (see Supporting Information) and 6-31G* basis sets for all the other atoms.[28]

Injection Mechanisms

In a simple electron donor−acceptor model, where an 8HQ molecule in the PS environment and the metal electrode represent the redox couple, we can calculate the electron and hole injection barriers, ϕ_e and ϕ_h, respectively. These are the Gibbs free energies required to transfer an electron from the aluminum electrode to an 8HQ molecule and vice versa:[9]

$$\phi_e = \phi_{Al} - EA \quad (1)$$

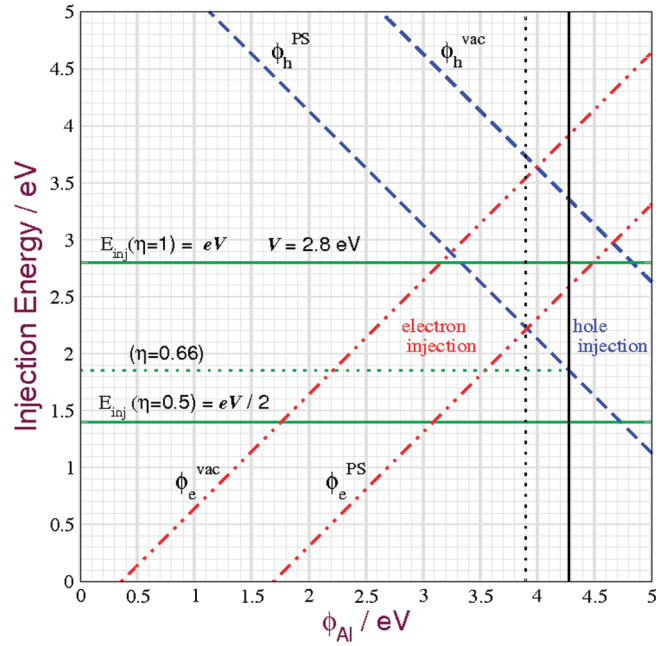

Figure 1. Electron (red curves) and hole (blue curves) injection barriers in vacuum and in PS, as a function of the aluminum work function. Green horizontal lines indicate the injection energies provided in some particular conditions (see text for explanation).

$$\phi_h = IP - \phi_{Al} \quad (2)$$

where ϕ_{Al} is the aluminum work function, and EA and IP are the 8HQ electron affinity and ionization potential, respectively. In the first part of this work,[8] the average experimental value of the bare aluminum work function[29] has been considered, and we calculated EA and IP of 8HQ in vacuum and solvated in amorphous polystyrene within the polarizable continuum model (see Table 6 in ref 8). At that level we neglected possible phenomena at the aluminum interface, such as molecular adsorption, or partial solvation of 8HQ molecules at boundaries, which could affect the injection barriers at zero bias, and the electric response under low voltage applications. In Figure 1 we show a plot of the electron and hole injection barriers in vacuum or in PS (red and blue lines, respectively), as a function of ϕ_{Al}. The lines of the calculated hole and electron injection barriers in PS intersect at the value $\phi_{Al} = 3.9$ eV (dotted black vertical line). For ϕ_{Al} values greater than 3.9 eV, the hole injection is favored, whereas the electron injection is preferred for smaller values. The injection energies E_{inj}, as provided under the application of 2.8 V bias, in the two limit cases of a symmetric ($\eta = 0.5$) or a totally asymmetric ($\eta = 1$) electric response at the interfaces, are sketched in green horizontal lines.[30,31] The asymmetry parameter η is a measure of the effective bias at the electrodes, and enters in the proportionality factor between the applied voltage (V) and the redox potentials (E_n) of the electrodes:

$$E_1 = \eta eV$$

$$E_2 = (\eta - 1)eV$$

where e is the electron charge. When $\eta = 0.5$, the electric responses of the two electrodes are symmetric, and the maximum energy disposal is $E_{inj} = |E_{1,2}| = 1.4$ eV for $V = 2.8$ V. Under these conditions, if the experimental average work

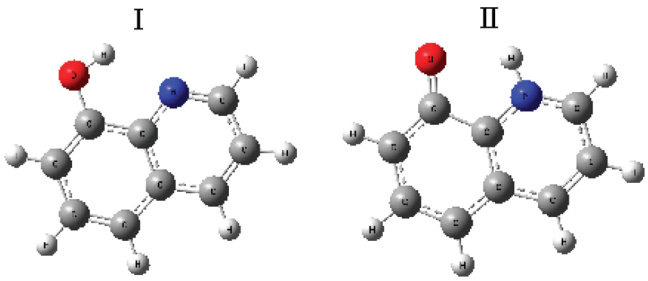

Figure 2. Enolic (I) and ketonic (II) tautomers of 8HQ.

function of a clean aluminum surface is considered ($\phi_{Al} = 4.28$ eV, black solid vertical line), the E_{inj} is not enough to inject either electrons or holes (see where the green horizontal line intersects with the black vertical line). Indeed, the hole (electron) injection barriers in PS lies 0.45 (1.2) eV higher in energy, and even much higher in vacuum. The only possibility to obtain hole injection with this particular value of ϕ_{Al}, is having $\eta \geq 0.66$, and even higher values for an electron injection.

Positive deviations of ϕ_{Al} from the bare aluminum value (4.28 eV) provide lower hole injection barriers (negative slope of ϕ_h) and higher electron injection barriers (positive slope of ϕ_e), which would endorse a hole-conduction mechanism. On the contrary, for negative variations of ϕ_{Al} larger than 0.3−0.4 eV, ϕ_e and ϕ_h intersect, and an injection inversion occurs, opening the possibility for electron-conduction mechanisms. The asymmetry parameter η can be determined if the ϕ_{Al} value and the solvation environment of 8HQ molecules are known.

8HQ Adsorption on Al (111)

The adsorption of the enolic (I) and ketonic (II) tautomers of 8HQ molecules (Figure 2) has been simulated by means of a 6-(3 × 3)-layer slab model. This particular arrangement simulates the formation of an adsorbed molecular monolayer on the surface, in a concentration which should grossly reproduce the average surface density of 8HQ molecules on the electrode surface in the memory device. The fully optimized structures have been found with periodic DFT/B3LYP calculations. We followed the Doll et al.[32] procedure to calculate improved metal work functions with localized basis sets, by adding basis functions in the vacuum region (ghost layers) above the metal surfaces at the same positions of the crystal lattice.

The optimized adsorption structures are shown in Figure 3a for the 8HQ(I), and in Figure 3b for the 8HQ(II) tautomers.

The 8HQ(I) molecules adsorb with the oxygen (nitrogen) atoms in the proximity of a top (hollow) site at a distance of 3.504 (3.791) Å from the first Al layer. The molecular plane is perpendicular to the Al surface (*xy* plane) and it forms a dihedral angle of 15° with respect to the *xz* plane. The Al surface structure remains essentially unchanged under molecular adsorption. The distance between the first and the second Al layer is expanded by just 0.03 Å with respect to the pristine Al slab (2.41 Å). From the analysis of the Mulliken charges, the aluminum slab retains some positive charge with an average depletion of about 0.08 *e* per surface aluminum atom. On the other hand, the 8HQ(I) molecule has also a little positive total charge of 0.18 *e*. The neutrality of the system is ensured by the two layers of ghost atoms which in turn have a negative charge of 0.046 *e* per ghost atom. Especially the first layer of ghost atoms which is closer to the aluminum slab and to the electronegative atoms of the 8HQ(I) is enriched by 0.092 *e* per ghost atom. Comparing the Mulliken charges between the isolated 8HQ(I) and the adsorbed 8HQ(I)/Al (111) at the same level of calculation, no relevant differences can be noticed. The modulus of the adsorbed 8HQ(I) Mulliken dipole moment is 3.89 D with respect to the molecular center of mass, without ghost atoms. This value is slightly larger than 3.35 D we calculated at the same level of calculation in gas phase. The dipole moment is oriented 41.2° from the normal to the Al surface, and it is directed toward the vacuum region.

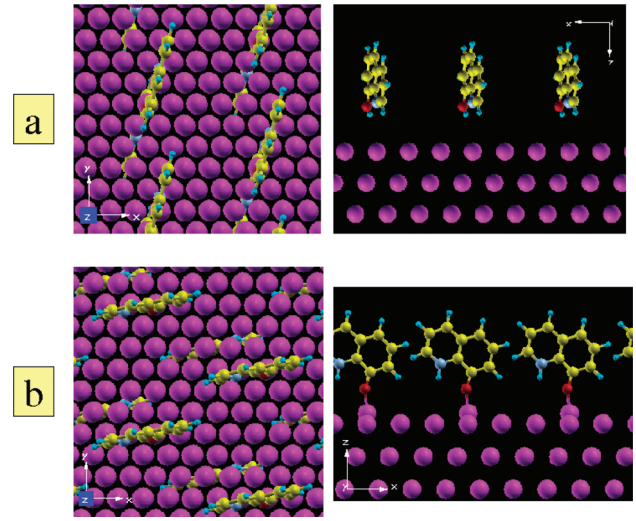

Figure 3. Periodic adsorption structure of (a) 8HQ(I) and (b) 8HQ(II) molecules on Al (111).

The 8HQ(II) molecules adsorb with the oxygen (hydrogen) atoms in the proximity of a top (bridge) site at a distance of 2.531 (3.441) Å from the first Al layer. The molecular plane is perpendicular to the Al surface (*xy* plane), and it forms a dihedral angle of 80° with respect to the *xz* plane. The Al atom which is closest to the O atom is pushed above the surface of 0.75 Å, forming an Al−O bond with a distance of 1.808 Å. In this case the first Al layer results to be compressed by 0.03 Å with respect to the bare Al surface, whereas the inner layers are slightly expanded. From the analysis of the Mulliken charges, the aluminum slab retains some positive charge with an average depletion of about 0.09 *e* per surface aluminum atom. The 8HQ(II) molecule has a tiny negative total charge of 0.019 *e*, whereas the two layers of ghost atoms have a total negative charge of 0.048 *e* per ghost atom. Especially the first layer of ghost atoms which is closer to the aluminum slab and to the electronegative atoms of the 8HQ(II) are enriched by 0.077 *e* per ghost atom. Comparing the Mulliken charges between the isolated 8HQ(II) and the adsorbed 8HQ(II)/Al (111) at the same level of calculation, the oxygen and the nitrogen atoms are slightly more negative by 0.09 and 0.08 *e*, respectively, when close to the Al surface. The modulus of the adsorbed 8HQ(II) Mulliken dipole moment, without ghost atoms, is 6.137 D with respect to the molecular center of mass. This value is quite similar to 6.124 D we calculated at the same level of calculation in gas phase, and to 6.245 D we calculated exactly from the DFT/B3LYP/N07D electron density of 8HQ(II) in gas phase.[8] The dipole moment is oriented 15.0° from the normal to the Al surface, and it is directed toward the vacuum region.

The adsorption energies are shown in Table 1, with and without ghost layers, expressed in kilocalories per adsorbed molecule. The ghost atoms play an important role also in the adsorption structures, and in the strength of adsorption bonds. When ghost layers are taken into account, the weak interaction of the enolic tautomer 8HQ(I) with the Al (111) surface is enhanced by 5.9 kcal (83%) per adsorbed molecule. In the 8HQ(II) adsorption, the ghost layers make the interaction

TABLE 1: Adsorption Energies of the Enolic and Ketonic Tautomers of the 8HQ Molecule on Different Al (111) Slab Models (with two ghost layers and without ghost layers), Expressed in Kilocalories per Adsorbed Molecule

	E_{ads} (without ghosts)	E_{ads} (two ghost layers)
8HQ(I)/Al (111)	−1.2	−7.1
8HQ(II)/Al (111)	−31.5	−36.3

TABLE 2: Al (111) Work Functions Calculated for the Clean Al (111) Surface and for the Two Adsorbed 8HQ Tautomers (with two ghost layers and without ghost layers)[a]

	ϕ_{Al}/eV (without ghost layers)	ϕ_{Al}/eV (two ghost layers)
Al (111)	2.92	3.76
8HQ(I)/Al (111)	2.86 (−0.06)	3.05 (−0.71)
8HQ(II)/Al (111)	2.39 (−0.53)	2.51 (−1.25)

[a] In parentheses are shown the work function variations with respect to the clean surface. Energies are in electronvolts.

between the molecule and the slab increase by 4.8 kcal (13%) per adsorbed molecule.

Table 2 shows the calculated work functions for the clean Al (111) surface, with the adsorbed 8HQ tautomers, with and without ghost layers. The Al (111) work function is lowered by the interaction with both the tautomers, but more when 8HQ(II) is adsorbed and when the ghost layers are employed.

In conclusion, our results indicate a possible lowering of the electrode work functions by up to 1.25 eV, due to the non-negligible interaction with 8HQ molecules present at the Al/PS interface. The related electron and hole injection barriers can hence be significantly decreased and increased, respectively (see Figure 1). The thermodynamics of the system is totally upset by the possible occurrence of 8HQ adsorption on the electrode surfaces, and the electron injection mechanism becomes the most probable.

Even more interesting is the possible role that molecular adsorption on the electrodes has on the bistability behavior of the memory device. The application of the bias could favor the tautomerization of the enolic 8HQ molecules to the ketonic form, whose a larger dipole moment allows a better alignment along the electric field and a more favorable adsorption on the electrode, with the consequent sharp decrease of the electron injection barrier. Furthermore, the asymmetric behavior of the $I-V$ plot could be caused by a large resistance to the inversion of the dielectric polarization under a reverse bias, due to the quite strong molecular adsorption of the ketonic 8HQ molecules.

Conclusions

Assuming an asymmetric electric response at the two aluminum electrodes, the voltage required to switch the device to a high-conductivity state could provide the hole injection energy, giving clues for a hole transport mechanism. However, only an explicit study of the electrode interfaces, which takes into account the adsorption of 8HQ molecules on the aluminum surfaces, opens the possibility to another sketch. The relevant decrease in the work function of the covered aluminum surface dramatically lowers (increases) the electron (hole) injection barrier, making the electron transport mechanism more probable to occur. Furthermore, a well-packed molecular adsorption would make the electron injection barrier accessible at 2.8 V, without invoking asymmetric electric behavior at the two electrodes.

The asymmetric features of the $I-V$ plot of the memory device could be due instead to the different relative stabilities of the 8HQ tautomers between the charged and the neutral molecules. Adiabatic electron transfers are likely to occur at the electrode interface where the 8HQ molecular structures would not vary in the time scale of the electron transfer event. At the same time, the later tautomerization reaction to the most stable ketonic structures of field-induced polarized molecules would change the molecular structures for the reversed charge transfer reaction. In this picture, in the "write" phase, when a positive bias is applied, the electron injection barriers would be larger than in the "erase" phase, when a negative bias is applied. For some reasons, possibly related to the charge stabilization role played by gold nanoparticles, the negatively charged 8HQ molecules would persist even after the electron injection, and would be neutralized only by a discharge reaction due to a reversed bias.

Acknowledgment. The work was funded from the PON 1575/2004 Project High Performance Cooperative Distributed System for Multidisciplinary Scientific Elaborations (S.Co.P.E. project from the Italian initials) and by MIUR (PO.DI.ME project). The VILLAGE network (http://village.unina.it) and CINECA are acknowledged for computational facilities.

Supporting Information Available: This material is available free of charge via the Internet at http://pubs.acs.org.

References and Notes

(1) Scott, J. C. *Science* **2004**, *304*, 62.
(2) Chen, Y.; Jung, G.-Y.; Ohlberg, D. A. A.; Li, X.; Stewart, D. R.; Jeppesen, J. O.; Nielsen, K. A.; Stoddart, J. F.; Williams, R. S. *Nanotechnology* **2003**, *14*, 462.
(3) Yang, Y.; Ouyang, J.; Ma, L.; Tseng, R.-H.; Chu, C.-W. *Adv. Funct. Mater.* **2006**, *16*, 1001.
(4) Paul, S. *IEEE Trans. Nanotechnol.* **2007**, *6*, 191.
(5) Muccini, M. *Nat. Mater.* **2006**, *5*, 605.
(6) Ouyang, J.; Chu, C.-W.; Szmanda, C.; Ma, L.; Yang, Y. *Nat. Mater.* **2004**, *3*, 918.
(7) Kwok, K. S.; Ellenbogen, J. C. *Mater. Today* **2002**, *5*, 28.
(8) Pino, I.; Sementa, L.; Causa, M.; Barone, V. *J. Phys. Chem. C* **2008**, *112*, 17081.
(9) Zaumseil, J.; Sirringhaus, H. *Chem. Rev.* **2007**, *107*, 1296.
(10) Singh, J. *Smart Electronic Materials*; Cambridge University Press: New York, 2005.
(11) Goodisman, J. *Electrochemistry: Theoretical Foundations*; Wiley-Interscience: New York, 1987.
(12) Schmickler, W. *Interfacial Electrochemistry*; Oxford University Press: New York, 1996.
(13) Scaldaferri, R.; Salzillo, G.; Pepe, G. P.; Barra, M.; Cassinese, A.; Pagliarulo, V.; Borriello, A.; Fusco, L. *Eur. Phys. J. B* **2009**, *72*, 113.
(14) Scaldaferri, R.; Bonavolontà, C.; Pepe, G. P.; Garzillo, G.; Borriello, A.; Pedaci, I. *Eur. Phys. J. B* **2010**, *73*, 207.
(15) Blyth, R. I. R.; Mittendorfer, F.; Hafner, J.; Sardar, S. A.; Duschek, R.; Netzer, F. P.; Ramsey, M. G. *J. Chem. Phys.* **2001**, *114*, 935.
(16) Ray, S. G.; Cohen, H.; Naaman, R.; Liu, H.; Waldeck, D. H. *J. Phys. Chem. B* **2005**, *109*, 14064.
(17) Heimel, G.; Romaner, L.; Brédas, J.-L.; Zojer, E. *Phys. Rev. Lett.* **2006**, *96*, 196806.
(18) Saunders, V. R.; Dovesi, R.; C., R.; Causa, M.; Harrison, N. M.; Zicovich-Wilson, C. M. *CRYSTAL '98 User Manual*; Turin University, Turin, Italy, 1999.
(19) Dovesi, R.; Saunders, V. R.; Orlando, R.; Zicovich-Wilson, C. M.; Pascale, F.; Civalleri, B.; Doll, K.; Bush, I. J.; D'Arco, P.; Lunell, M. *Crystal 2006 User Manual*; Turin University: Turin, Italy, 2007.
(20) Dovesi, R.; Pisani, C.; Roetti, C.; Saunders, V. R. *Phys. Rev. B* **1983**, *28*, 5781.
(21) Causà, M.; Dovesi, R.; Orlando, R.; Pisani, C.; Saunders, V. R. *J. Phys. Chem.* **1988**, *92*, 909.
(22) Pisani, C.; Dovesi, R.; Roetti, C. *Lecture Notes in Chemistry*; Springer-Verlag: Heidelberg, Germany, 1988.
(23) Zicovich-Wilson, C. M.; Dovesi, R. *Int. J. Quantum Chem.* **1998**, *67*, 299.
(24) Doll, K.; Harrison, N. M.; Saunders, V. R. *Int. J. Quantum Chem.* **2001**, *82*, 1.
(25) Doll, K. *Comput. Phys. Commun.* **2001**, *137*, 74.

(26) Civalleri, B.; D'Arco, P.; Orlando, R.; Saunders, V. R.; Dovesi, R. *Chem. Phys. Lett.* **2001**, *348*, 131.
(27) Becke, A. D. *J. Chem. Phys.* **1993**, *98*, 5648.
(28) Hehre, W. J.; Ditchfield, R.; Pople, J. A. *J. Chem. Phys.* **1972**, *56*, 2257.
(29) Eastment, R. M.; Mee, C. H. B. *J. Phys. F* **1973**, *3*, 1738.
(30) Tian, W.; Datta, S.; Hong, S.; Reifenberger, R.; Henderson, J. I.; Kubiak, C. P. *J. Chem. Phys.* **1998**, *109*, 2874.
(31) Adams, D. M. *J. Phys. Chem. B* **2003**, *107*, 6668.
(32) Doll, K. *Surf. Sci.* **2006**, *600*, L321.

JP1063287